Geomechanics and Engineering, *Vol. 32, No. 6 (2023) 601-613*
https://doi.org/10.12989/gae.2023.32.6.601

Experimental study on modified low liquid limit silt for abutment backfill in bridge-embankment transition section

Shu-jian Wang[1,2], Yong Sun[1], Zhen-bao Li[1,3], Kai Xiao[4] and Wei Cui*[5]

[1]*Geotechnical and Structural Engineering Research Center, Shandong University, Jinan 250061, China*
[2]*Shandong Hi-speed Group CO., Ltd., Jinan 250101, China*
[3]*Research Institute of New Material and Intelligent Equipment, Shandong University, Dezhou 251100, China*
[4]*Shandong Luqiao Group CO., Ltd., Jinan 250021, China*
[5]*School of Qilu Transportation, Shandong University, Jinan 250002, China*

(*Received May 19, 2022, Revised February 18, 2023, Accepted February 19, 2023*)

Abstract. Low liquid limit silt, widely distributed in the middle and down reaches of Yellow River, has the disadvantages of poor grading, less clay content and poor colloidal activity. It is very easy to cause vehicle jumping at the bridge-embankment transition section when the low liquid limit silt used as the backfill at the abutment back. In this paper, a series of laboratory tests were carried out to study the physical and mechanical properties of the low liquid limit silt used as back filling. Ground granulated blast furnace slag (GGBFS) was excited by active MgO and hydrated lime to solidify silt as abutment backfill. The optimum ratio of firming agent and the compaction and mechanical properties of reinforced soil were revealed through compaction test and unconfined compressive strength (UCS) test. Scanning electron microscope (SEM) test was used to study the pore characteristics and hydration products of reinforced soil. 6% hydrated lime and alkali activated slag were used to solidify silt and fill the model of subgrade respectively. The pavement settlement regulation and soil internal stress-strain regulation of subgrade with different materials under uniformly distributed load were studied by model experiment. The effect of alkali activated slag curing agent on curing silt was verified. The research results can provide technical support for highway construction in silt area of the Yellow River alluvial plain.

Keywords: bridge-subgrade transition section; GGBFS; low liquid limit silt; model test; solidified silt; vehicle jumping

1. Introduction

Pile foundation is usually adopted as the foundation of the bridge of expressways. The settlement of pile foundation of bridge is usually less than that of the embankment, which leads to differential settlement in bridge-embankment transition section and vehicle bumping at bridge head, especially when the high embankment backfill or large traffic load. In general, there are three types of vehicle bumping at bridge head: (1) The settlement is caused by the consolidation and compression of the subgrade under self-weight and vehicle load, and the differential settlement of bridge-embankment transition section occurs under the condition of abutment back fill without approach slab, leading to vehicle bumping at bridge head (see Fig. 1(a)); (2) The local depression of backfill soil near the abutment occurs due to the loss of backfill soil under vehicle load and water scouring, resulting in vehicle bumping at bridge head (see Fig. 1(b)); and (3) The motion of one end of approach slab near the abutment occurs due to the settlement of abutment back fill and subgrade, leading to vehicle bumping at bridge head. The vertical displacement of the other end of approach slab is caused by the redistribution of traffic load on the approach slab, resulting in secondary vehicle bumping (see Fig. 1(c)). Moreover, vehicle bumping at bridge head will be aggravated when the approach slab fractures during long-term operation of expressway. There are many hazards caused by vehicle bumping at bridge head (e.g., noise pollution to the surrounding residents, decline of road traffic efficiency, threaten of driver or passenger life safety, and damage of expansion joints, bearings and approach slabs), when vehicle passes through the bridge-embankment transition section. In practice, a large amount of maintenance funds (e.g., the cost of the replacement of approach slab and the reinforcement of backfill) is needed to avoid vehicle bumping at bridge-embankment transition section of expressway.

Alluvial (silting) soil layer is widely distributed in the plains of the Yellow River in China. The alluvial soil layer is mostly silty soil with low clay content, poor colloidal activity, high roundness and poor particle grading, leading to be difficult to be compacted (Xiao *et al*. 2008, Xu *et al*. 2010). During the construction of expressway in the plains of the Yellow River, the alluvial soil is often used as the filling soil at the abutment back considering the project cost and the lack of sand. The subgrade and the abutment back fill may have large post construction settlement under traffic dynamic load and subgrade gravity, and vehicle bumping at bridge-embankment transition section of expressway is often observed in the plains of the Yellow River. Therefore, the soil in the plains of the Yellow River

*Corresponding author, Professor
E-mail: cuiwei01@sdu.edu.cn

Copyright © 2023 Techno-Press, Ltd.

ISSN: 2005-307X (Print), 2092-6219 (Online)

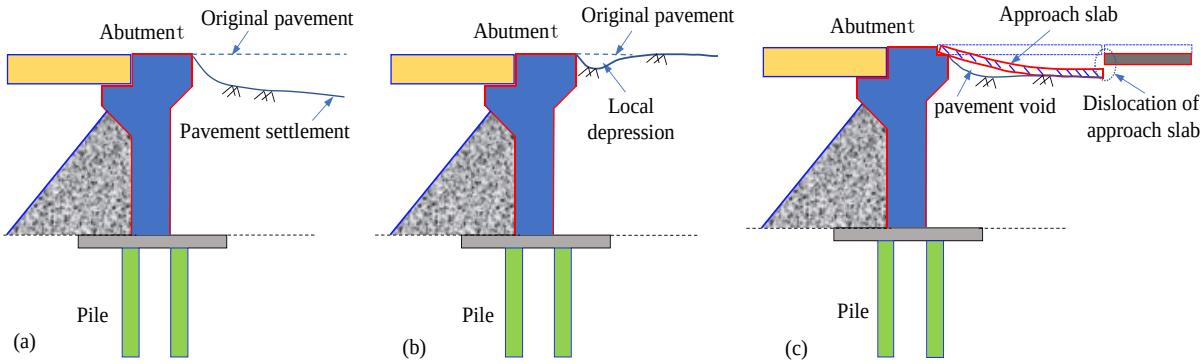

Fig. 1 Types of vehicle bumping at bridge head: (a) Overall settlement of abutment back fill without approach slab, (b) Loc al settlement of abutment back fill without approach slab and (c) Settlement between bridge-head and abutment back fill wi th approach slab

used as fill materials of abutment back must be reinforced in practice.

The traditional curing agents such as cement, hydrated lime and fly ash are widely used to reinforce the alluvial and silting soil layers in the plains of the Yellow River in China. Xu *et al*. (2010) carried out a series of laboratory experiments to analyze the UCS of solidified silt mixed with fly ash, lime and slag powder under different curing times. Jumassultan et al. (2021) study on the UCS of calcium sulfoaluminate cement reinforced sand under different curing conditions. Yao *et al*. (2007) studied the flexural, freezing stability and water stability of the silt solidified by hydrated lime using laboratory experiments. Lo *et al*. (2002) analyzed the shear properties and dilatancy effect of cement and fly ash reinforced silt by using triaxial tests. The previous researches shows that due to the lack of clay in silt and the weak cementation effect, the strength, water stability and freezing stability of the silt solidified by hydrated lime is low. The silt solidified by hydrated lime and fly ash have not been widely used in practice because of large dosage (e.g., the optimum content is more than 30%), high cost and low early strength. The silt solidified by cement can greatly improve the water and freezing stability, however, the UCS of the silt solidified by cement is low, and the dry and temperature shrinkage of the silt solidified by cement are often observed. It is well known that during the production of cement and hydrated lime, a large amount of energy will be consumed and a great quantity of carbon dioxide (CO_2) is discharged, e.g., the production of 1.0 t cement needs to consume about 5000 MJ of energy and emit about 0.95 t of CO_2, while the production of 1.0 t hydrated lime needs to consume about 3200 MJ of energy and emit about 0.79 t of CO_2 (Shand, 2006).

For practical purposes, GGBFS is a by-product of iron and steel industry, which can be used to reinforce silt with the advantages of hydraulic activity, green environmental protection and low price (Zabihi *et al*. 2019). Wang *et al*. (2006) analyzed the unconfined saturated compression, water stability, freezing stability, and dry shrinkage of silt solidified by GGBFS using laboratory experiments. The test results showed that the soil specimens solidified by GGBFS were immersed in water for 1 day after curing for 6 days, and all the specimens were disintegrated and damaged in water, indicating that GGBFS was unable to form enough hydration products to bond the silt particles together in a short time. Therefore, some kinds of alkaline activator e.g., NaOH solution, water glass, hydrated lime, and active MgO, should be added to accelerate the hydration rate of GGBFS and improve the early strength of the soil solidified by GGBFS. Zhou *et al*. (2020) studied the reinforcement principle and microstructure of bentonite-containing reinforcement materials by laboratory test and SEM test. Thomas *et al*. (2020) carried out laboratory experiments to investigate the influence of nano-silica particles in the consistency limits, compressive strength of the soft clay blended with cement. Sharma *et al*. (2016) analyzed the Atterberg limits, compaction characteristics and unconfined compressive strength of expansive soils reinforced by fly ash and GGBFS. Thomas *et al*. (2018) carried out laboratory experiments to study the UCS and shear strength of clay reinforced by cement and GGBFS activated by NaOH solution. Gu *et al*. (2015) analyzed the strength of clay modified with GGBFS activated by hydrated lime and active MgO. Yi *et al*. (2015) analyzed the mechanism of clay reinforced by GGBFS activated by active MgO and hydrated lime using scanning electron microscope (SEM) and X-ray diffraction tests.

The previous researches mainly focus on the characteristics of loose silt and clay reinforced by Alkali activated GGBFS, and there is rare research on the characteristics of silt reinforced by GGBFS activated with Alkali. In this paper, the laboratory tests were carried out to study the physical and mechanical properties of the low liquid limit silt used as bench back filling, and the optimal content of firming agent was determined by compaction test and UCS test. The shear strength characteristics of reinforced soils was determined by using triaxial shear test, and the hydration product characteristics of firming agent and pore characteristics of reinforced soil were determined by SEM test. The model tests were carried out to capture the displacement and stress of the solidified silt (e.g., reinforced by Alkali activated GGBFS and hydrated lime) used as backfill of bridge-embankment transition section. The reinforcement effect of low liquid limit silt modified by curing agent is verified. The research results can provide

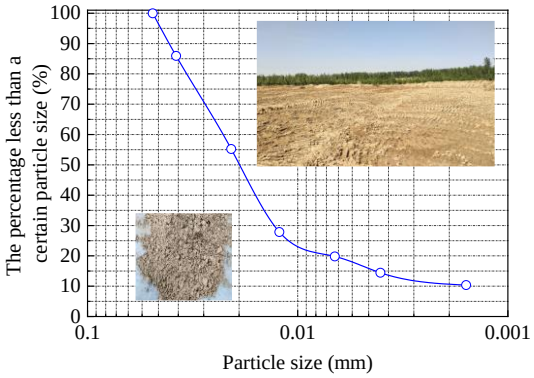

Fig. 2 Particle grading curve of the soil

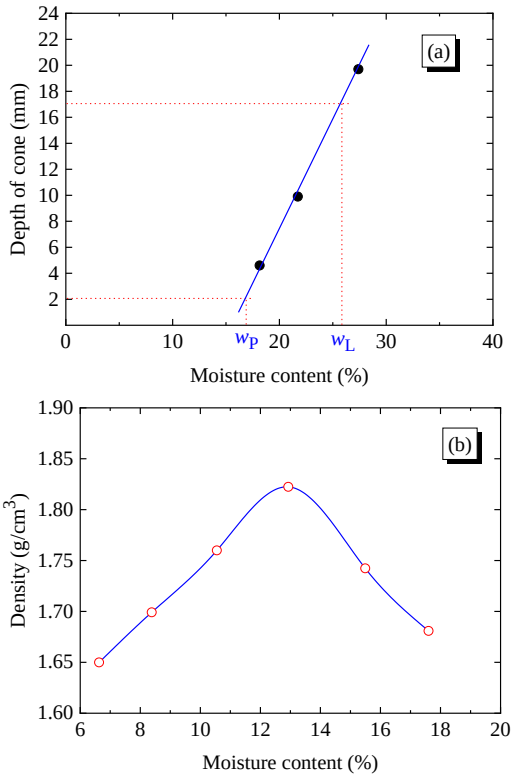

Fig. 3 Physical properties of the soil: (a) Liquid and plastic limit and (b) Optimum moisture content and maximal dry density

technical support for highway construction in silt area of the Yellow River alluvial plain.

2. Physical and mechanical properties of silt

The soil specimens were taken from the Yellow River alluvial plain, Shandong Province, China, and were placed in the sampling box to maintain the moisture content. According to Chinese Test Methods of Soils for Highway Engineering (JTG 3430-2020), a series of laboratory tests were carried out to determine the gradation, liquid plastic limit, optimal water content, maximum dry density, shear strength and compression shrinkage coefficient of soil. The particle analysis result of the soil is shown in Fig. 2.

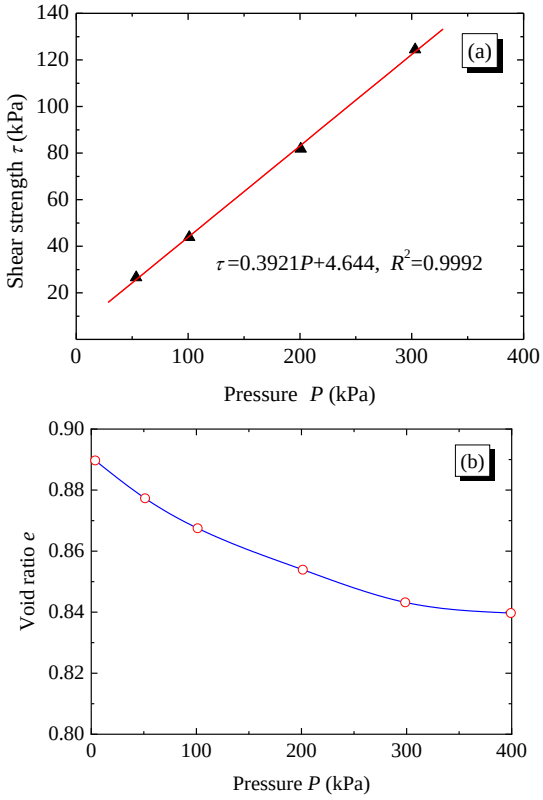

Fig. 4 Mechanical properties of the low liquid limit silt: (a) Shear strength and (b) Compression coefficient

Fig. 2 shows that the clay content (i.e., the particle size is smaller than 0.002 mm), the silt content (i.e., the particle size is in the range of 0.002 to 0.075 mm) and the sand content (i.e., the particle size is in the range of 0.075 to 2 mm) in the selected soil are about 10.6 %, 89.4 %, and 0, respectively. The non-uniformity coefficient C_u of the soil specimen is calculated as 16.7 and the curvature coefficient C_c is adopted as 6. Therefore, the soil taken from the Yellow River alluvial plain can be considered as poorly graded soil.

Fig. 3 shows that the liquid limit w_L and the plastic limit w_P of the soil are 25.9% and 16.4%, respectively, and the plastic index I_P is taken as 9.5. The soil can be named low liquid limit silt. The maximum dry density of the low liquid limit silt is 1.82 g/cm^3 and the optimum moisture content is 12.9%.

The mechanical properties of low liquid limit silt obtained from the laboratory tests are shown in Fig. 4.

Fig. 4(a) shows that the internal friction angle of the low liquid limit silt is 21.4°, and the cohesion of the low liquid limit silt is 4.64 kPa. Fig. 4(b) shows that the compression coefficient of the low liquid limit silt $\alpha_{1\text{-}2}$ can be calculated as 0.136 MPa^{-1}, suggesting that the low liquid limit silt is medium compression soil (0.1 MPa^{-1}<$\alpha_{1\text{-}2}$<0.5 MPa^{-1}).

3. Laboratory test of solid silt

As previously mentioned, the silt solidified by the traditional firming agents (e.g., cement, lime and fly ash) cannot be meet the requirements of as abutment backfill,

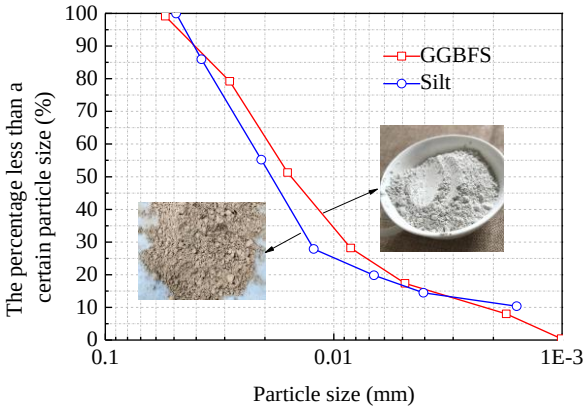

Fig. 5 Particle grading curves of GGBFS and silt

Fig. 6 Active MgO

and the production process of traditional firming agents consumes a lot of energy and resources. GGBFS is a by-product of iron and steel industry, and can be used to reinforce silt with the advantages of hydraulic activity, green environmental protection and low price (Abdila *et al*. 2022, Keramatikerman *et al*. 2016). The hydration rate of GGBFS needs to be excited by alkaline activator, such as sodium silicate, NaOH solution, hydrated lime and active MgO. The soil reinforced by GGBFS with sodium silicate as alkaline activator is not meet the time requirement for subgrade filling due to the fact that sodium silicate condenses too fast in the subgrade construction. NaOH solution can effectively activated GGBFS, however, NaOH solution is inconvenient to use in construction as an aqueous solution. Therefore, sodium silicate and NaOH solution do not meet the requirements of solidified silt as abutment backfill. Hydrated lime and active MgO in powder form can effectively activate GGBFS with a moderate hydration rate, and can be used as the activator of GGBFS. Therefore, this paper focuses on the physical and mechanical properties of silt reinforced by GGBFS with hydrated lime and active MgO as alkaline activator.

3.1 Test material and test method

GGBFS is made of slag by ball milling to a certain particle size and has an activity grade of S95. The particle grading curves of GGBFS and low liquid limit silt are shown in Fig. 5.

Fig. 5 shows that the distribution of particle size of GGBFS and silt is similar. The silt content of GGBFS is more than 90%, and the grading is slightly better than that of the low liquid limit silt.

Active MgO with activity grade of MA 150 is a new type of alkaline activator of GGBFS, and is white powder (see Fig. 6).

The main chemical composition of GGBFS, MgO and hydrated lime is summarized in Table 1.

The proportion of reinforced soil and test scheme are summarized in Table 2: (1) The UCS tests on the reinforced soil specimens with maximum dry density of 1.82 g/cm^3 were carried out to capture the optimum ratio of active MgO to GGBFS, where the mass ratio of firming agent to dry soil was adopted as 0.15 and the mass ratio of active MgO to GGBFS was taken as 0.1, 0.2, 0.3 and 0.4, respectively;

Table 1 Main chemical composition of GGBFS, MgO and hydrated lime

Ingredient	Proportion (%)		
	GGBFS	MgO	Hydrated lime
$Ca(OH)_2$	-	-	97.21
$CaCO_3$	-	-	0.72
CaO	34.00	0.7	-
SiO_2	34.30	0.4	0.61
Al_2O_3	17.90	-	0.03
SO_3	1.64	-	-
Fe_2O_3	1.02	0.6	0.04
MgO	6.02	>98	0.27
K_2O	0.64	-	-
TiO_2	1.17	-	-
Loss on ignition	2.67	2.0	-

(2) The UCS tests on the reinforced soil specimens with compactness of 94% were carried out to capture the optimum content of alkaline activator, where the mass ratio of alkali activator to GGBFS was adopted as 0.15 and the mass ratio of GGBFS to dry silt soil was taken as 0.03, 0.06, 0.09, 0.12, 0.15, 0.18, 0.21, and 0.30, respectively; (3) The triaxial shear test on the reinforced soil specimens with compactness of 94% were carried out to assess the shear characteristics of the reinforced soil, where the content of alkaline activator was adopted as 6% and 15%, and the content of hydrated lime was taken as 6% using as the control group; and (4) The SEM tests on the soil specimens reinforced by GGBFS activated with hydrated lime and active MgO (the content of firming agent was 6% and 15%, respectively) were carried out to investigate the pore characteristics and hydration products of the reinforced soil.

3.2 Analysis on test results

The relationship between maximum dry density and optimum moisture content of the reinforced soil is shown in Fig. 7.

Fig. 7 shows that the maximum dry density of the soil reinforced by GGBFS activated with active MgO gradually

Table 2 Proportioning and test scheme of the soil

Test No.	Mass ratio of firming agent to dry soil	Mass ratio of alkaline activator to GGBFS	Test scheme
1	0.15	0.1, 0.2, 0.3, 0.4	UCS test
2	0.03, 0.06, 0.09, 0.12, 0.15, 0.18, 0.21, 0.30	0.15	Compaction test, UCS test
3	0.06，0.15	0.15	Triaxial shear test
4	0.06，0.15	0.15	SEM test

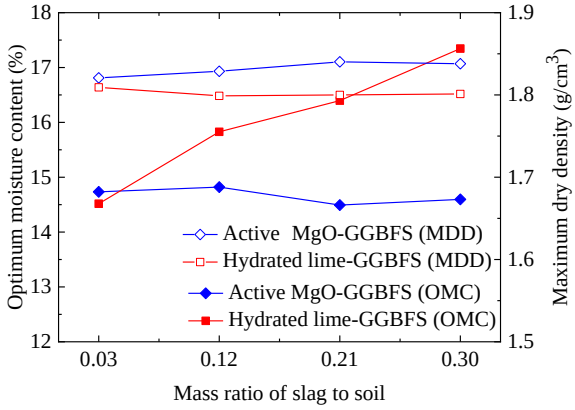

Fig. 7 Relationship between maximum dry density and optimum moisture content of the reinforced soil

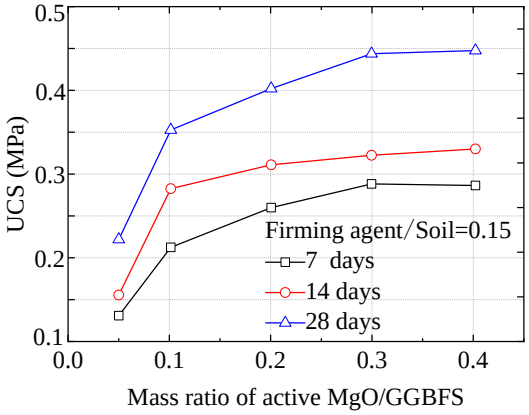

Fig. 9 Influence of mass ratio of active MgO to GGBFS on the UCS of the reinforced soil specimen

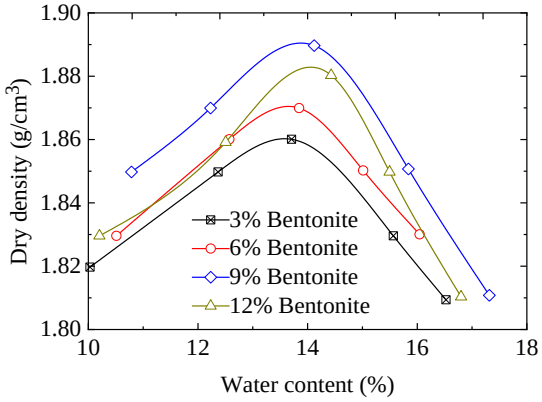

Fig. 8 Influence of clay content on maximum dry density and optimum water content of soil specimens

increases with increasing firming agent content, while the maximum dry density of the soil reinforced by GGBFS activated with hydrated lime slightly decreases with increasing firming agent content. However, the firming agent content has little effect on the maximum dry density of the reinforced soil, because the particle grading of GGBFS and silt is approximately the same (see Fig. 5). The silt content in GGBFS accounts for more than 80%, and the content of active MgO used for filling the pores among silt particles accounts for only 0.45% to 4.5% of the quality of reinforced soil, leading to the lack of fine particles for filling the pores among silt particles in the reinforced soil. To improve the compaction performance of the reinforced soil, an appropriate amount of clay can be added to the alkali-activated slag reinforced soil. As to the soil reinforced by GGBFS activated with hydrated lime, the optimum moisture content increases gradually with increasing firming agent, while the optimum moisture content of the soil reinforced by GGBFS activated with active MgO slightly decreases with increasing firming agent content. This is due to the fact that hydrated lime has strong water absorption (Mleza *et al*. 2012), while active MgO shows hydrophobicity (Zehra *et al*. 2022).

Fig. 8 shows the compaction test results of low liquid limit silt mixed with bentonite accounting for 3%, 6%, 9% and 12% of dry soil mas, respectively.

It can be seen from Fig. 8 that the maximum dry density of the reinforced soil specimen increases with increasing bentonite content for the bentonite content in the range of 3% to 9%, and decreases when the bentonite content increases from 9% to 12%. It can be concluded that the optimal content of bentonite is within the range of 9% to 12%.

The influence of mass ratio of active MgO to GGBFS on the UCS of the reinforced soil specimen is shown in Fig. 9.

Fig. 9 shows that the UCS of the reinforced soil specimen increases with increasing mass ratio of active MgO to GGBFS and curing age, and the increasing rate decreases with increasing mass ratio of active MgO to GGBFS. When the content of active MgO increases, more Mg2+ and OH- will be produced in the reinforced soil (see Eq. (1)), leading to the increase of pH value in the reinforced soil and more main hydration products (e.g., calcium silicate hydrate (C-S-H), see Eq. (2)) in high alkaline environment. The hydration products will fill the pores among soil particle and cement soil particles, resulting in a high early strength of the soil specimen. When the content of active MgO is too high, the surface of soil particles will be adsorbed by a large amount of non-hydrolyzed active MgO, leading to the decrease of friction among soil particles. This is the reason that the increasing

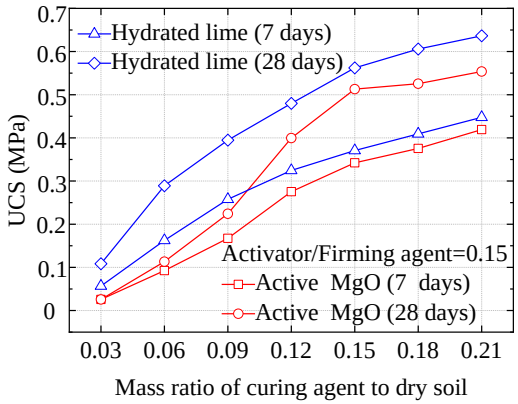

Fig. 10 Influence of GGBFS content on UCS of the reinforced soil specimen

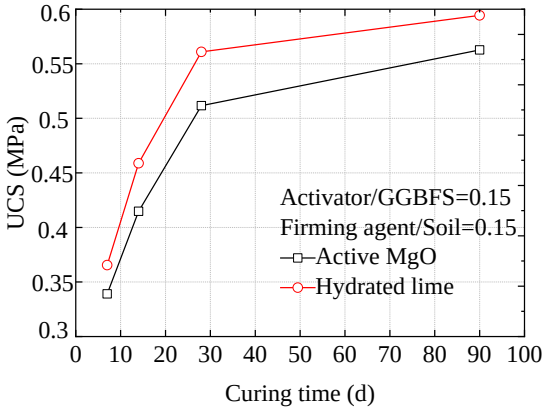

Fig. 11 Relationship between UCS of the reinforced soil specimen and curing time

rate of UCS of the reinforced soil specimen is not obvious under high mass ratio of active MgO to GGBFS. Considering economy and characteristics of hydration reaction, it is necessary to consume small amount of active MgO to ensure the excitation efficiency of GGBFS. Therefore, the optimal mass ratio of active MgO to GGBFS can be taken as 0.15 to 0.20.

$$Mg(OH)_2+H_2O\rightarrow Mg^{2+}+OH^- \quad (1)$$

$$CaO\text{-}MgO\text{-}Al_2O_3\text{-}SiO_2(slag)+Mg(OH)_2+H_2O\rightarrow CSH+\ CASH \quad (2)$$

The influence of GGBFS content on UCS of the soil specimens reinforced by GGBFS activated with active MgO and hydrated lime is shown in Fig. 10.

Fig. 10 shows that the UCS of the soil specimen reinforced by GGBFS activated with active MgO increases with increasing content of firming agent. The 7-day UCS of the reinforced soil specimen with active MgO content of 9% is 0.16 MPa, which meets the strength requirement of reinforced soil. The increasing of 28-day UCS of the reinforced soil specimen changes comparatively small, when the content of activated MgO exceeds 15%. Therefore, the optimum content of GGBFS activated by active MgO can be taken as 15%. As to the soil specimen reinforced by GGBFS activated with hydrated lime, the increasing rate of UCS of the reinforced soil specimen decreases with increasing firming agent content. The 7-day and 28-day UCS of the soil specimens reinforced by GGBFS activated with active MgO are smaller than that of the soil specimens reinforced by GGBFS activated with hydrated lime. The 7-day UCS of the soil specimen reinforced by GGBFS activated with hydrated lime content of 6% (e.g., 0.17 MPa) can meet the strength requirement of reinforced soil.

The relationship between UCS of the reinforced soil specimen and curing time is shown in Fig. 11.

Fig. 11 shows that when the GGBFS content is 15%, the UCS of the reinforced soil specimen increases with increasing curing time. Under different curing times, the UCS of the soil specimen reinforced by GGBFS activated with hydrated lime are larger than that of the soil specimen reinforced by GGBFS activated with active MgO. The hydrated degree of GGBFS activated by hydrated lime is higher than that of GGBFS activated by active MgO, therefore, the early strength of the soil specimen reinforced by GGBFS activated with hydrated lime is large. The hydration of the GGBFS is the main cause of long-term strength of the reinforced soil, however, the alkaline activator only accelerates the hydration reaction process (Yi *et al*. 2015). This is the reason that there is little difference in long-term UCS between the soil reinforced by GGBFS activated with hydrated lime and the soil reinforced by GGBFS activated with active MgO.

3.3 Triaxial shear test on the reinforced soil specimen

A series of triaxial shear tests on the reinforced soil specimen with dry density of 1.82 g/cm^3 were carried out to get shear strength of the reinforced soil. The scheme of triaxial shear test on the reinforced soil specimen is summarized in Table 3, in which the dry specimen was cured in the standard curing environment for 28 days, and the wet specimen was the dry specimen cured for 28 days and immersed in water for 1 day.

The cohesion of the reinforced soil specimens with different firming agents is shown in Fig. 12.

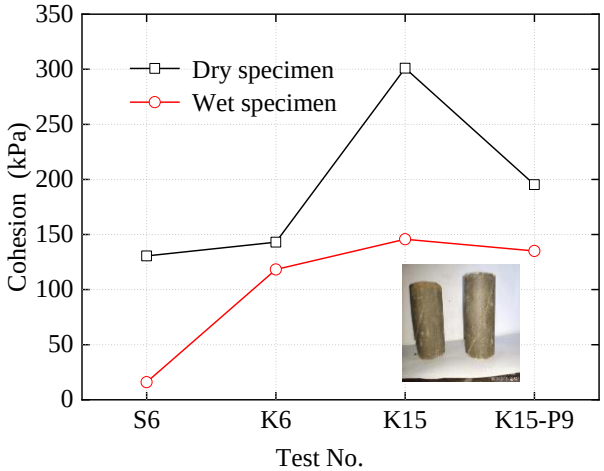

Fig. 12 Cohesion of the reinforced soil specimens with different firming agents

Table 3 Scheme of triaxial shear test on the reinforced soil specime

Test No.	Firming agent	Dry and humidity conditions
S6-g	6% hydrated lime	Dry specimen
S6-s	6% hydrated lime	Wet specimen
K6-g	GGBFS activated by 6% active MgO	Dry specimen
K6-s	GGBFS activated by 6% active MgO	Wet specimen
K15-g	GGBFS activated by 15% active MgO	Dry specimen
K15-s	GGBFS activated by 15% active MgO	Wet specimen
K15-P9-g	9% Bentonite and GGBFS activated by 15% active MgO	Dry specimen
K15-P9-p	9% Bentonite and GGBFS activated by 15% active MgO	Wet specimen

Fig. 12 shows that the cohesion of the reinforced soil specimen K6-g is slightly larger than that of the reinforced soil specimen S6-g, indicating that the reinforcement effect of GGBFS is better than that of hydrated lime under the same content of firming agent. The cohesion of the dry reinforced soil specimen obviously increases from 130.5 kPa to 301.0 kPa, when the content of GGBFS increases from 6% to 15%. As previously stated, network hydration products C-S-H can improve the cohesion and compactness of the reinforced soil specimen, and the content of C-S-H increases with increasing content of GGBFS. The cohesion of the reinforced soil specimen K15-P9-g (e.g., 195.3 kPa) is smaller than that of the reinforced soil specimen K15-g. Therefore, bentonite can improve the compactness of the reinforced soil, and reduce the cohesion of the reinforced soil.

The cohesion of the reinforced soil specimen S6-s decreases from 130.5 kPa to 15.9 kPa after the reinforced soil specimen is soaked in water for 1 day. The content of clay particles in the low liquid limit silt is small (see Fig. 2, less than 11%), and there are few active Al_2O_3 and SiO_2 in the low liquid limit silt. Therefore, the pozzolanic reaction between hydrated lime and silt is very weak, as shown in Eqs. (3) and (4). The carbonation and crystallization of $Ca(OH)_2$ in hydrated lime are poor, resulting in low initial strength and poor water resistance of the soil specimen reinforced by hydrated lime. In practice, the strength of the subgrade filled with the silt solidified by hydrated lime will significantly decrease under the condition of rainfall or rising groundwater level, leading to the instability of subgrade (Qin *et al*. 2001). After immersion in water, the cohesion of the silt solidified by GGBFS activated with active MgO will also decrease, however, the cohesion of the silt solidified by GGBFS activated with active MgO is larger than that of the soil solidified by hydrated lime. This indicates that the water stability of the silt solidified by GGBFS activated with active MgO is better than that of the silt solidified by hydrated lime.

$$Ca(OH)_2+CO_2+nH_2O\rightarrow CaCO_3\downarrow+(n\text{-}1)H_2O \quad (3)$$

$$Ca(OH)_2+nH_2O\rightarrow Ca(OH)_2\cdot nH_2O \quad (4)$$

The internal friction angle of the reinforced soil specimens with different firming agents is shown in Fig. 13.

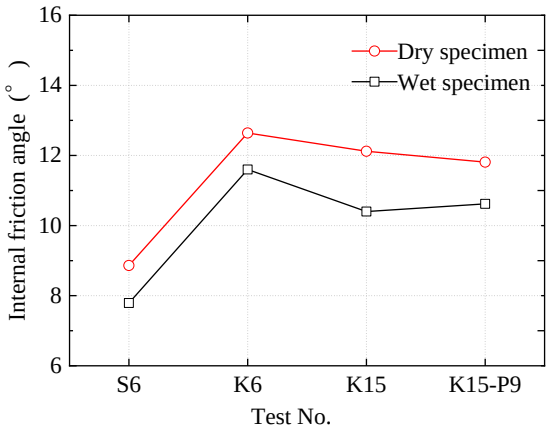

Fig. 13 Internal friction angle of the reinforced soil specimens with different firming agents

Fig. 13 shows that the internal friction angle of the wet reinforced soil specimen is smaller than that of the dry reinforced soil specimen, and the internal friction angle of the dry specimen solidified by GGBFS activated with active MgO is significantly larger than that of the soil solidified by hydrated lime. The internal friction angle of the reinforced soil reduces when the content of GGBFS increases from 6% to 15%. The internal friction angle of the reinforced soil further reduces when 9% bentonite is added in the reinforced soil. Therefore, the internal friction angle of the reinforced soil will be reduced due to the addition of bentonite and high content of GGBFS.

3.4 Micro characteristics of the materials

The reinforced soil was made into test specimen with a dry density of 1.82 g/cm^3 and cured in a standard curing environment for 90 days. The reinforced soil specimen was crushed to fragments with a diameter of less than 10 mm and lyophilized with liquid nitrogen, and then placed in a vacuum environment for 48 hours. The improved silt fragments were observed by using SEM, as shown in Fig. 14, where the mass ratio of active MgO or hydrated lime to GGBFS was 0.15, and the mass ratio of firming agent to dry soil was 0.06 and 0.15, respectively.

Active MgO is formed by calcination of magnesite crystal at about 700°C, and has a porous structure with large specific surface area and adsorption capacity (see Fig. 14(a)), indicating that active MgO has high activity. Fig. 14(b) shows that GGBFS particles is multi ribbed particles with smooth surface, while active MgO particles is a crystal with porous structure. The diameter of active MgO particles is much smaller than that of GGBFS particles, about 0.05 to 0.2 times diameter of GGBFS particles. Figs. 14(c) and (d) show that the hydration products of GGBFS activated by active MgO and hydrated lime are different. The hydration products of GGBFS activated by active MgO are only gas-soluble colloidal (C-S-H, see Eq. (2)), while the hydrated products of GGBFS activated by hydrated lime include gas-soluble colloidal (C-S-H) and acicular ettringite crystals ($3CaO\cdot Al_2O_3\cdot 3CaSO_4\cdot 32H_2O$, which is the main product of cement hydration). During the formation of ettringite, a

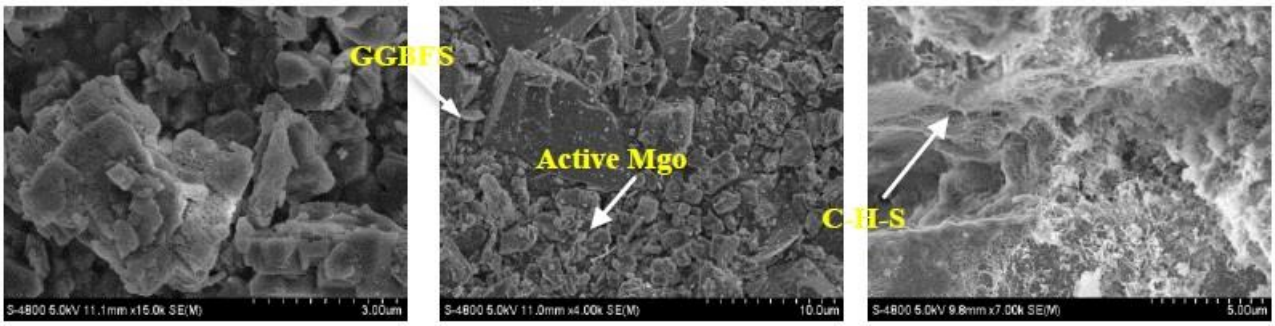

(a) Powder of active MgO (b) Powder of active MgO and GGBFS (c) Hydration products of active MgO and GGBFS

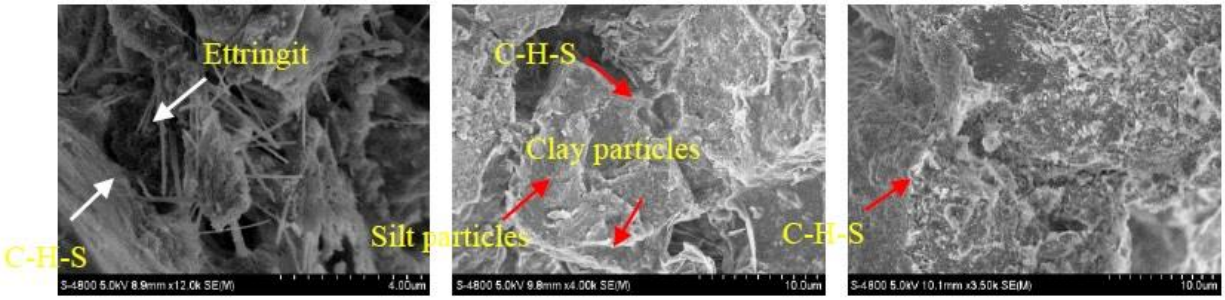

(d) Hydration products of hydrated lime and GGBFS (e) Content of 3% curing agent (Active MgO) (f) Content of 15% curing agent (Active MgO)

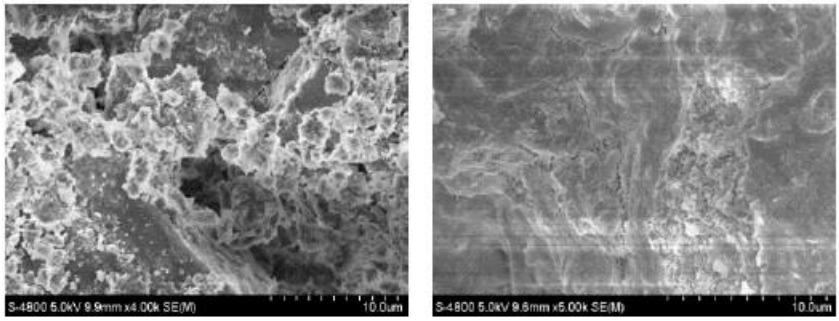

(g) Content of 3% curing agent (Hydrated lime) (h) Content of 15% curing agent (Hydrated lime)

Fig. 14 SEM image of the materials

large amount of free water will be fixed to form bound water, and ettringite crystals can fill the pores among particles. This is the reason that the early strength of the soil specimen reinforced by GGBFS activated with hydrated lime is larger than that of the soil specimen reinforced by GGBFS activated with active MgO (see Figs. 10 and 11). The content of generated ettringite shall be compatible with the porosity of the compacted silt, and excessive ettringite will lead to cracking of the reinforced soil and reducing of the reinforced soil strength. Therefore, the content of hydrated lime should be controlled in a reasonable range. Figs. 14(e)-14(h) show that the amount of C-S-H aerosols on the surface of silt particles is small and a large number of pores still exist among particles when the content of firming agent is 3%. When the content of firming agent increases to 15%, the surface of silt particles is wrapped by the hydration products of C-S-H, and the pores among particles are filled with hydration products, leading to the compactness of solidified silt and the improvement of reinforced soil strength.

4. Model test of subgrade filled using solidified silt

The above-mentioned research shows that the UCS of the silt solidified by alkali activated GGBFS is significantly improved, comparing with the silt solidified by 6% hydrated lime commonly used in practice. Therefore, the stability of subgrade in backfill area can be improved and the settlement of backfill subgrade can be reduced when the silt solidified by alkali activated GGBFS is used as abutment backfill. To verify the reinforcement effect of GGBFS activated by alkali on the silt, model tests were carried out. In the model tests, the silt solidified by 6% hydrated lime and GGBFS activated with alkali were used to fill the subgrade, respectively, and the pavement settlement and the stress-strain relationship of subgrade under uniformly distributed load were studied.

4.1 Test materials

Low liquid limit silt and low liquid limit silt solidified

(a) Silt sieved using a sieve

(b) Firming agent and silt fully mixed

(c) Optimum moisture content dertemined

Fig. 15 Preparation method of test materials

(a) Steel chamber

(b) Control cabinet

(c) Hydraulic pump

(d) Hydraulic jack

Fig. 16 Large multifunctional loading test system

by firming agent were used in the model tests. The firming agent used in the model tests was GGBFS with the activity grade of S95 and active MgO with active magnesium oxide of MA 150.

The treatment process of low liquid limit silt used in model test is summarized as following:

(1) The low liquid limit silt was pass through a sieve with mesh size of 5 mm to screen out stones, sundries and large particle soil blocks.

(2) The initial moisture content of the silt was determined using combustion method, and the optimum moisture content of the silt was determined according to the compaction test results.

(3) The amount of water needed was determined according to the optimum moisture content of the silt, and the water was uniformly sprayed to the surface of the silt using a sprinkler. During the process of watering, the silt was continuously mixed using a shovel to ensure uniform mixing of the silt.

(4) The moisture content of the silt was determined by combustion method after watering. If the moisture content was insufficient, repeat the above steps and continue to add water until the optimum moisture content of the silt was obtained.

The treatment process of the reinforced soil is similar to that of the silt. During the test, a certain quality of GGBFS and activator was weighed according to the test ratio, and fully mixed with the silt to get the optimum moisture content of the reinforced silt (see Fig. 15).

4.2 Test equipment

A self-developed large-scale multifunctional loading test system (Liu *et al*. 2021, Feng *et al*. 2020) was used including model frame, steel chamber, loading system controller and data acquisition computer, as shown in Fig. 16. The model frame was a steel frame structure connected by high-strength bolts. The steel chamber with a dimension of 3 m×3 m×3 m was placed on two steel beams, and could be freely moved along the lead rail through rollers to easily fill soils. To conveniently observe the soil filling process, one side of the fill chamber was made of transparent toughened glass and reinforced by a steel frame.

The hydraulic loading system included control cabinet, hydraulic pump and hydraulic jack. Hydraulic jack with a maximum loading capacity of 200 kN and a loading accuracy of 0.5 N was fixed to the crossbeam using linear bearings and could be moved freely. The control cabinet consisted of computer, supporting software and hydraulic oil pump control circuit board. The loading system could be uniformly load according to the set loading rate, and the load could be automatically maintained.

4.3 Instrumentation and layout

The model test was carried out to study the compression and strength characteristics of two types of abutment backfill material, e.g., the silt solidified by 6% hydrated lime and GGBFS activated with alkali. The subgrade model

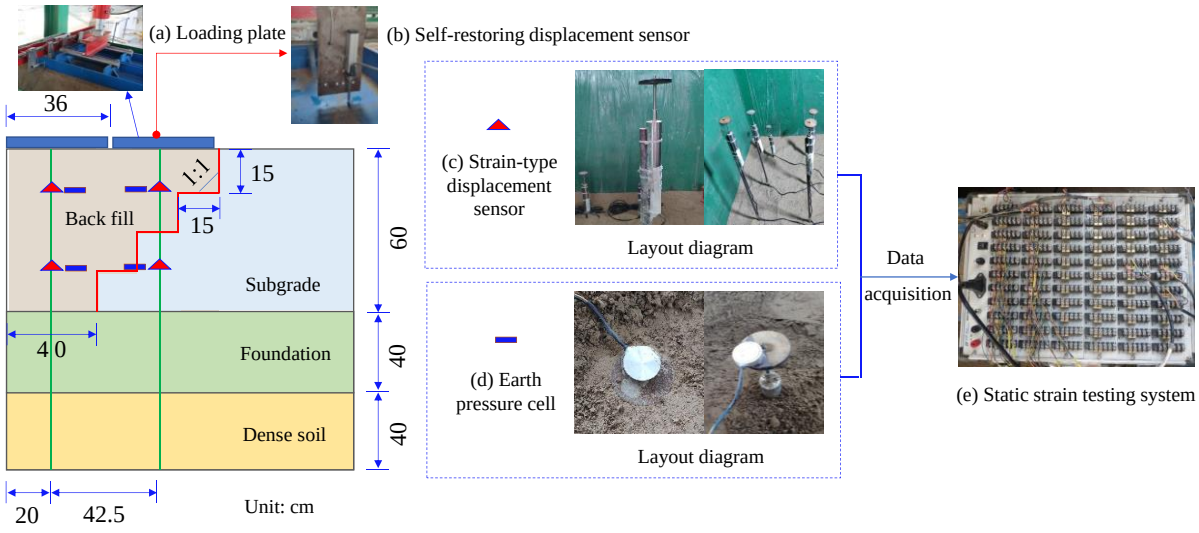

Fig. 17 Layout diagram of instrumentations

in the test was simplified as follows: (1) The subgrade slope was not set in the test, ignoring the influence of subgrade slope; and (2) The influence of highway surface was not considered.

A split loading plate capable (see Fig. 17(a)) was designed to apply uniform load. The loading plate was made of steel plate with a thickness of 1.5 cm to ensure the stiffness of the system. A round bar with a diameter of 5 cm was welded on the upper part of the loading plate. The I-beam was placed in the middle of the two round bars to ensure free movement of the two loading plates. Two loading plates were placed at the backfill of abutment back and the junction between backfill soil and subgrade, respectively. When differential settlement of subgrade model existed, the loading plate could move and keep in horizontal level to ensure uniformly applied load.

Self-restoring displacement sensor with an effective stroke of 50 mm and an accuracy of 0.05 mm was used to capture the displacement of backfill surface (see Fig. 17(b)). Strain-type displacement sensor with a measure range of 0~50 mm and a sensitivity coefficient of 100~120 με/mm was used to get displacement at different depths of backfill and subgrade (see Fig. 17(c)). A steel base was fixed at the bottom of the steel chamber, and the telescopic rod was connected to the steel base using threads. A series of settlement plate embedded in the backfill and subgrade at a specific depth were installed at the telescopic rod, and the strain-type displacement sensors were connected to the settlement plates. The displacement at different depths of backfill and subgrade was measured according to the movement of the settlement plate transmitted through the telescopic rod. Micro earth pressure cell glued on the settlement plate was used to measure the earth pressure of different depths of backfill and subgrade (see Fig. 17(d)).

The micro earth pressure cell had a measure range of 0~200 kPa and a sensitivity coefficient of 0~10 με/mm. Static strain test system was used to obtain the measured data of strain-type displacement sensor and micro earth pressure cell (see Fig. 17(e)). The static strain test system had 60 channels with an acquisition accuracy of 0.1 uε and an acquisition frequency of 2 Hz. Using the data acquisition software, real-time acquisition, processing and recording of data could be achieved.

4.4 Experiment process

The experiment process was summarized as follows:

(1) Fix the connecting rod at the bottom of the steel chamber, and install the strain-type displacement sensors according to the design height (see Fig. 18(a)).

(2) Place 40 cm sand in the steel chamber with filling height of each layer of 10 cm, and compact the sand layer by layer (see Fig. 18(b)).

(3) Fill the low liquid limit silt on the sand layer with filling height of each layer of 10 cm and total height of 40 cm as foundation (see Fig. 17). To ensure that the compactness of foundation reached 90% during the filling of each layer, ring knife method was used to detect the compactness of foundation (see Fig. 18(c)).

(4) Fill the low liquid limit silt on the foundation with filling height of each layer of 10 cm and total height of 60 cm as subgrade (see Fig. 17). To ensure that the compactness of subgrade reached 94% during the filling of each layer, ring knife method was used to detect the compactness of subgrade (see Fig. 18(d)).

(5) After the overall filling of the subgrade was completed, the steps at the back of the subgrade were excavated according to the size requirement of Fig. 17, as shown in Fig. 18 (d).

(6) Fill the reinforced soil in the excavation area following the filling method of the subgrade. The compactness of the reinforced soil (e.g., the soil solidified by GGBFS activated with active MgO and the soil solidified by hydrated lime) was controlled to 94%. At the layout height of settlement plate and earth pressure cell (glued on the settlement plate, see Fig. 18(e)), the floating soil under the settlement plate was cleaned to ensure that the settlement plate was in close contact with the lower soil

(a) Install strain-type displacement sensors

(b) Backfill and compact sand

(c) Backfill and compact silt

(d) Renovate the steps

(e) Paste earth pressure cell on settlement plate

(f) Install split loading plate capable

(g) Apply loading

(h) Install self-restoring displacement sensor

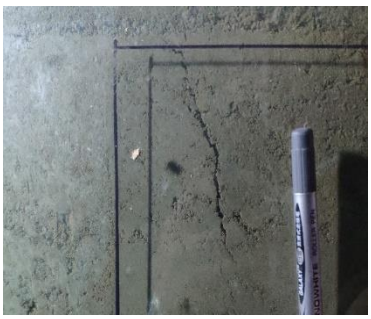

(i) Terminate loading

Fig. 18 Experiment process

layer.

(7) The reinforced soil was cured for 28 days after backfilling to make the curing agent fully hydrated.

(8) The split loading plate capable was placed on the reinforced soil after curing of the reinforced soil (see Fig. 18(f)). The loaded was applied using the loading system with a loading rate of 20 kN/h (see Fig. 18(g)), and the strain acquisition instrument was used to continuously collect the data of instruments (see Fig. 18(h)).

(9) Stop loading when cracks appeared in the soil (see Fig. 18(i)).

4.5 Analysis on the test results

Under the load of 148 kPa, cracks were observed in the soil, and the load was stopped. The relationship between applied stress and displacement of soil at different depths is shown in Fig. 19, where point 1-1 and point 2-1 represent the monitoring points 15 cm away from the top surface in the backfill soil solidified by hydrated lime and GGBFS activated with active MgO, respectively, and point 1-3 and point 2-3 represent the monitoring points 45 cm away from the top surface in the backfill soil solidified by hydrated lime and GGBFS activated with active MgO, respectively.

Fig. 19(a) shows that the settlement of the soil at different depths in the backfill area increases with increasing stress, however, the settlement rate decreases gradually. Under the stress of 148 kPa, the maximum settlement of point 1-1 and point 1-3 are 3.36 mm and 1.59 mm, respectively, and the settlement difference between point 1-1 and point 1-3 is 1.77 mm. The maximum settlement of point 2-1 is 0.864 mm, which is smaller than that of point 1-1. The settlement difference between point 1-1 and point 2-1 increases with the increase of stress level.

Fig. 19(b) shows that the settlement of the soil at different depths in the junction of backfill area and subgrade increases with increasing stress, however, the settlement rate decreases gradually. Under the stress of 148 kPa, the maximum settlement of point 1-1 and point 1-3 are 6.79 mm and 2.88 mm, respectively. The maximum settlement of point 2-1 is 3.11 mm, which is smaller than that of point 1-1, e.g., the settlement difference between

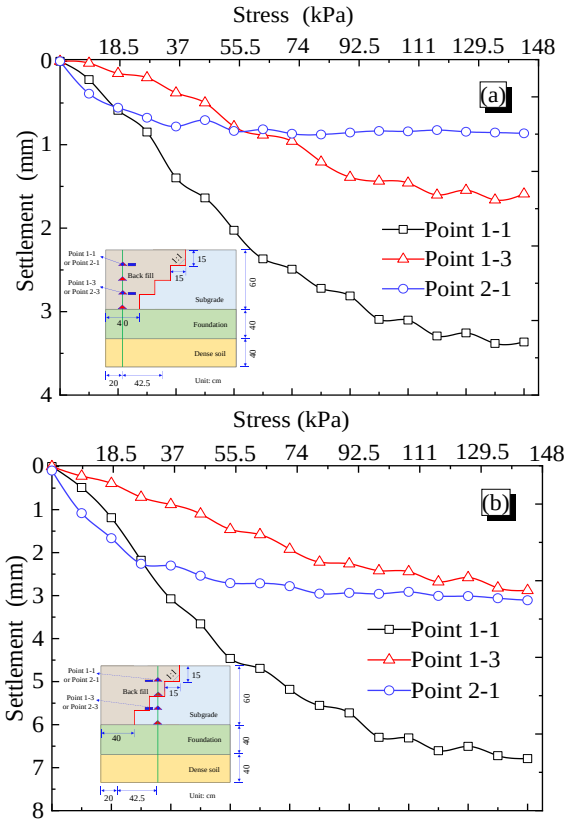

Fig. 19 Relationship between stress and displacement of soil at different depths: (a) Backfill area and (b) Junction of backfill area and subgrade

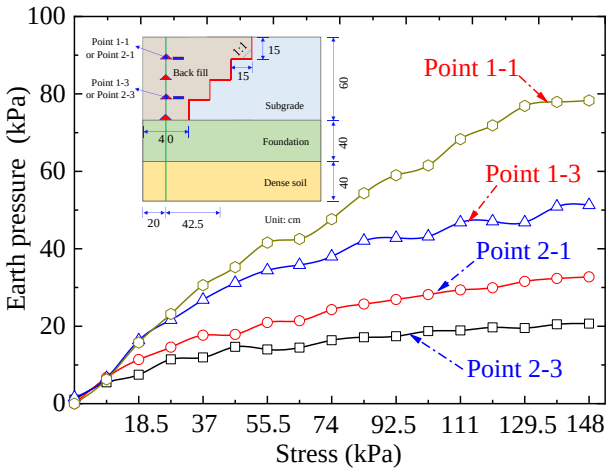

Fig. 20 Variation of earth pressure of the reinforced soil in the backfill area

point 1-1 and point 2-1 is 3.68 mm. The soil settlement at the junction of the backfill area and the subgrade is larger than that at the backfill area. The upper and lower part of the soil at the junction is reinforced soil and low liquid limit silt, respectively, which is beneficial to reduce the differential settlement of transition section. For the silt solidified by GGBFS activated with active MgO, the compressive modulus and cohesion can be obvious improved due to the bonding and filling effect of hydration products. This is the reason that the maximum settlement of the silt solidified by GGBFS activated with active MgO (e.g., point 2-1) is obviously smaller than that solidified by hydrated lime (e.g., point 1-1) at the same depth. It can be concluded that the silt solidified by GGBFS activated with active MgO, used as the backfill of abutment back, has obvious advantages over the silt solidified by hydrated lime in reducing the differential settlement of road-bridge transition section in practice.

Fig. 20 shows the earth pressure of the reinforced soil in the backfill area.

It can be seen from Fig. 20 that the earth pressure is smaller than the applied load due to stress diffusion, and decreases with increasing depth. At the same depth, the earth pressure of the soil reinforced by GGBFS activated with active MgO is obviously smaller than that reinforced by hydrated lime. As above-mentioned analysis, the compressive and shear strength of the soil reinforced by GGBFS activated with active MgO is larger than that reinforced by hydrated lime. The stress diffusion of the soil reinforced by GGBFS activated with active MgO is more obvious than that reinforced by hydrated lime, resulting in a rapid reduction of earth pressure with increasing depth in the soil reinforced by GGBFS activated with active MgO.

5. Conclusions

This paper presents a series of laboratory tests to study the physical and mechanical properties of the low liquid limit silt used as bench back filling, and the optimal content of firming agent was determined by using compaction test and UCS test. The shear strength of the reinforced soil was determined by using triaxial shear test, and the hydration product characteristics of firming agent and pore characteristics of reinforced soil were determined by using SEM test. The model tests were carried out to capture the displacement and stress of the solidified silt used as backfill of bridge-embankment transition section under uniformly distributed load. The main conclusions are summarized as follows:

- The silt has poor grading and can be regarded as medium compression soil. The low liquid limit silt in the plains of the Yellow River used as fill materials of abutment back must be reinforced in practice. The content of clay in the low liquid limit silt is small, leading to a weak pozzolanic reaction with hydrated lime. The low liquid limit silt is not suitable for reinforce with hydrated lime.
- The maximum dry density of silt can be slightly increased by adding GGBFS activated with active MgO, which is conducive to improve the mechanical properties and durability of the reinforced soil. The maximum dry density of silt can be slightly reduced by adding GGBFS activated with hydrated lime.
- The UCS of the reinforced soil increases with increasing content of firming agent. The best activator of GGBFS is active MgO, and the optimum content of active MgO is 15% of the mass of GGBFS. The compaction of the reinforced soil can be improved by adding bentonite, and the optimal content of bentonite is 9% to 12%.
- The cohesion and internal friction angle of the reinforced soil can be improved by adding GGBFS activated with

active MgO. The water resistance of the soil reinforced by GGBFS activated with active MgO is better than that reinforced by hydrated lime. Compared with the soil reinforced by hydrated lime, the soil reinforced by GGBFS activated with active MgO has obvious advantages in reducing differential settlement of bridge-embankment transition section.

Acknowledgements

This work was supported by the Young Experts of Taishan Scholar Project of Shandong Province (No. tsqn202103163), the National Natural Science Foundation of China (No. 52078278, No. 51778345), and the program of Qilu Young Scholars of Shandong University. Great appreciation goes to the editorial board and the reviewers of this paper.

References

Abdila, S.R., Abdullah, M.M., Ahmad, R., Nergis, D.D.B., Rahim, R.S.A., Omar, M.F., Sandu, A.V. and Vizureanu, P. (2022). "Potential of soil stabilization using Ground Granulated Blast Furnace Slag (GGBFS) and fly ash via geopolymerization method: A review", *Mater.*, **15**(1), 375. http://doi.org/10.3390/ma15010375.

Feng, R.F., Zhang, Q.Q. and Liu, S.W. (2020). "Experimental study of the effect of excavation on existing loaded piles", *J. Geotech. Geoenviron.*, **146**(9), 04020091. http://doi.org/10.1061/(ASCE)GT.1943-5606.0002336.

Gu, K., Jin, F., Al-Tabbaa, A., Shi, B., Liu, C. and Gao, L. (2015), "Incorporation of reactive magnesia and quicklime in sustainable binders for soil stabilization", *Eng. Geol.*, **195**, 53-62. http://doi.org/10.1016/j.enggeo.2015.05.025.

JTG 3430-2020 (2020), Test methods of soils for highway engineering, Ministry of Transport of the People's Republic of China; Beijing, China.

JTG D30-2019 (2019), Specifications for Design of Highway Subgrade, Ministry of Transport of the People's Republic of China; Beijing, China.

Jumassultan, A., Sagidullina, N., Kim, J., Ku, T. and Moon, S.W. (2021) "Performance of cement-stabilized sand subjected to freeze-thaw cycles", *Geomech. Eng.*, **25**(1), 41-48. https://doi.org/10.12989/gae.2021.25.1.041.

Keramatikerman, M., Chegenizadeh, A. and Nikraz, H. (2016), "Effect of GGBFS and lime binders on the engineering properties of clay", *Appl. Clay Sci.*, **132**(1), 722-730. http://doi.org/10.1016/j.clay.2016.08.029.

Liu, S.W., Zhang, Q.Q. and Feng, R.F. (2021), "Model test study on bearing capacity of non-uniformly arranged pile groups", *Int. J. Geomech.*, **21**(10), 04021200. http://doi.org/10.1061/(ASCE)GM.1943-5622.0002181.

Lo, S.R. and Wardani, S.P. (2002), "Strength and dilatancy of a silt stabilized by a cement and fly ash mixture", *Can. Geotech. J.*, **39**(1), 77-89. http://doi.org/10.1139/T01-062.

Mleza, Y. and Hajjaji, M. (2012), "Microstructural characterisation and physical properties of cured thermally activated clay-lime blends", *Constr. Build. Mater.*, **26**(1), 226-232. https://doi.org/10.1016/j.conbuildmat.2011.06.014.

Qin, L.S. and Zheng, J.L. (2001), "Analysis of surficial failure mechanism of expansive soil slops with FEM", *China J. Highw. Transp.*, **14**(1), 25-30. http://doi.org/10.19721/j.cnki.1001-7372.2001.01.006.

Shand, M.A. (2006), The chemistry and technology of magnesia. Wiley & Sons, New Jersey.

Sharma, A.K. and Sivapullaiah, P.V. (2016), "Ground granulated blast furnace slag amended fly ash as an expansive soil stabilizer", *Soils Found.*, **56**(2), 205-212. http://doi.org/10.1016/j.sandf.2016.02.004.

Thomas, A., Tripathi, R.K. and Yadu, L.K. (2018). "A laboratory investigation of soil stabilization using enzyme and alkali-activated ground granulated blast-furnace slag", *Arab. J Sci. Eng.*, **43**(10), 5193-5202. https://doi.org/10.1007/s13369-017-3033-x.

Thomas, G. and Rangaswamy, K. (2020), "Strengthening of cement blended soft clay with nano-silica particles", *Geomech. Eng.*, **20**(6), 505-516. https://doi.org/10.12989/gae.2020.20.6.505.

Wang, Z.J., Weng, Y.L. and Du, S.W. (2006), "Theoretical analysis and field performance of silt soil reinforced with slag powder", *J. Eng. Geo.*, **14**(5), 709-714. http://doi.org/1004-9665/2006/14(05)-0709-06(in Chinese with English Abstract).

Xiao, J.H., Liu, J.K., Peng, L.Y. and Chen, L.H. (2008), "Effects of compactness and water Yellow-River alluvial silt content on its mechanical behaviors", *Rock Soil Mech.*, **29**(2), 409-414. http://doi.org/10.16285/j.rsm.2008.02.043(in Chinese with English Abstract).

Xu, D.S. (2010). "Research on mechanical characteristics and strengthen method of silt in Yellow River delta", Master's thesis of Institute of Rock & Soil Mechanics Chinese Academy of Sciences, China. (in Chinese with English Abstract).

Yao, Z.Y., Lian, J.J., Ai, Y.Z. and Shang, Q.S. (2007), "Compaction properties on Yellow River silty soil stabilized with lime-flyash", *Chin. J. Geotech. Eng.*, **29**(5), 664-670. http://doi.org/1000-4548(2007)05-0664-07(in Chinese with English Abstract).

Yi, Y.L., Gu, L.Y. and Liu, S.Y. (2015), "Microstructural and mechanical properties of marine soft clay stabilized by lime-activated ground granulated blastfurnace slag". *Appl. Clay. Sci.*, **103**, 71-76. http://doi.org/10.1016/j.clay.2014.11.005.

Zabihi, S.M. and Tavakoli, H.R. (2019), "Evaluation of monomer ratio on performance of GGBFS-RHA alkali-activated concretes", *Constr. Build. Mater.*, **208**, 326-332. http://doi.org/10.1016/j.conbuildmat.2019.03.026.

Zehra, T. and Kaseem, M. (2022), "Recent advances in surface modification of plasma electrolytic oxidation coatings treated by non-biodegradable polymers", *J. Mol. Liq.*, **365**, 120091. https://doi.org/10.1016/j.molliq.2022.120091.

Zhou, F., Sun, W.B., Shao, J.L., Kong, L.J. and Geng, X.Y. (2020) "Experimental study on nano silica modified cement base grouting reinforcement materials", *Geomech. Eng.*, **20**(1), 67-73. https://doi.org/10.12989/gae.2020.20.1.067.

CG